Effect of hadron dynamics on the proton lifetime

Alfred Scharff Goldhaber*
C.N. Yang Institute for Theoretical Physics, State University of New York, Stony Brook, New York 11794-3840

T. Goldman† and Richard R. Silbar‡
Theoretical Division, Los Alamos National Laboratory, Los Alamos, New Mexico 87545
(Received 6 June 2002; published 6 September 2002)

A detailed, quantitative reexamination of the effect of hadron dynamics on baryon decay, modeled in terms of Skyrme-field tunneling, indicates that any hadronic suppression should be quite mild. This appears to be another illustration of the ''Cheshire-cat'' phenomenon, that variation of the apportionment between description of the nucleon as a bag of quarks and description as a Skyrme field configuration has little influence on many nucleon properties. Perhaps the largest remaining uncertainty in evaluating the decay rate has to do with the overlap between a specified quark-antiquark configuration and a final meson state.

DOI: 10.1103/PhysRevD.66.056001 PACS number(s): 11.30.Fs, 12.39.Ba, 12.39.Dc, 13.30.Eg

I. INTRODUCTION

There is a limited number of known ways to seek physics beyond the standard model of electroweak and strong interactions. Increasing collision energies in laboratory experiments might reveal new particles. There may be small effects or rare processes at low energies. There might be particles of such high mass that they could not be created in the laboratory but have survived from an early, high-temperature epoch in the universe. Recently there has been evidence for new physics in the second category: the strong experimental indication of neutrino flavor oscillations, which imply small but nonzero neutrino masses [1,2]. This evidence encourages further pursuit of other phenomena, including proton decay, which, like neutrino mass, is not forbidden by some established principles such as gauge invariance.

During a period of (unsuccessful) search for baryon number non-conservation in large underground detectors, the question arose whether the rearrangement of hadronic degrees of freedom required for decay might substantially inhibit the process. It was suggested that such ''hadronic quenching'' might account for several orders of magnitude suppression of baryon decay [3]. Recent theoretical studies guided by the neutrino masses and by the assumption of ''grand unification'' of electroweak and strong interactions at some high scale have led to new predictions of baryon decay, involving different dominant channels from those first discussed, and smaller coefficients for the effective four-fermion operators generating the decay [4]. Evidently, if there were several orders of magnitude further suppression due to hadron dynamics, the prospects for experimental observation would be dim. Accordingly, it seems timely to make a more systematic and quantitative approach to the issue of hadronic suppression, and we attempt that here.

In principle one would like to carry out a path-integral computation over the QCD degrees of freedom, starting with a nucleon and ending with a meson and lepton. However, this remains a daunting task, because there is such poor quantitative control on the properties of QCD in exactly this regime, phenomena involving energy scales of the same order as $\Lambda_{\mathrm{QCD}} \approx 0.2$ GeV. Therefore, as in the earlier work, we use instead Skyrme's ansatz [5] for the nucleon as a topological soliton of the chiral field, and to provide more microscopic realism we allow a bag to occupy the interior region of the Skyrmion, with three valence quarks inside it. This is the hybrid chiral bag model [6]. To describe hadronic tunneling in the initial $B=1$ and final $B=0$ states, we take a single collective variable, the value of the chiral angle at the bag boundary radius R, where, for the Skyrmion in equilibrium, the angle would be $\pi/2$, halfway between the values 0 at spatial infinity and π at the origin. We estimate the tunneling action by using the Skyrme ansatz throughout space, constraining the ansatz by imposing varying values for the chiral angle at R.

Assuming that the formulation is exactly correct in every respect except that we are restricting the tunneling to only the single variable of the chiral angle at the fixed boundary of the bag, the result of this calculation should be a lower bound on the hadronic matrix element of the four-fermion operator which reduces baryon and lepton numbers each by one unit. It is a lower bound because taking account of more degrees of freedom should only increase the tunneling probability, barring cancellations due to opposing phases.

In our earlier work [3] it was suggested from crude dimensional considerations that the tunneling between a final, trivial vacuum state and a configuration of the chiral field with topological number zero but mass equal to the nucleon mass could be equivalent to the motion of a particle with GeV mass through a GeV potential barrier of thickness about 1 fm. This immediately gives a suppression factor 10^{-2} in amplitude or 10^{-4} in rate. Tunneling in the initial $B=1$ state was ignored. What we find now is that both the initial and final state tunneling factors are relatively large, meaning that the Skyrme ansatz indicates a soft degree of freedom associated with change of the chiral angle at the bag radius, either for fluctuations about the vacuum as in the final state (which consists of vacuum plus a departing meson and lepton), or

*Email address: goldhab@insti.physics.sunysb.edu
†Email address: t.goldman@post.harvard.edu
‡Email address: silbar@lanl.gov

 ©2002 The American Physical Society

for fluctuations about the $B=1$ initial state.

Put differently, quantum fluctuations of the vacuum are easily generated in which objects appear which consist of a quarter Skyrmion outside the radius R and a quarter anti-Skyrmion inside (or vice versa). In addition, fluctuations of a Skyrmion are easily generated in which one quarter of the baryon number shifts inside (or outside) the radius R. These are not the only modifications from a traditional (MIT bag [7]) estimate of baryon decay. Because the radius of the chiral bag boundary is about half that of the MIT bag, one must pay attention to the dimensional dependence of the four-fermion-operator matrix element on the volume which bag wave functions of quarks occupy. Also, the wave functions for the valence quarks take a different form as the chiral boundary angle varies from the case for chiral boundary angle 0, as in the MIT bag.

All these effects are taken into account in what follows. We begin by defining the matrix element to be estimated, then determine the initial and final state tunneling factors, and end by putting in factors for the initial quark and final meson and lepton wave functions. It will be seen that the calculation is nearly identical for the old dominant channel, $p\to e^+\pi^0$, and for the channel favored in more recent calculations $p\to\bar{\nu}K^+$, except for the larger mass and hence lower final velocity of K compared to π, and the gamma matrices appearing in the four-fermion operator, neither of which alters the hadronic tunneling. Our conclusion is that, because of the large spontaneous chiral fluctuations, hadronic tunneling implies at most a quite minor suppression of baryon decay.

II. THE DECAY MATRIX ELEMENT

The proton decay amplitude for $p\to m\bar{l}$ in terms of initial and final state wave functions $\Psi_{\rm final}$ and $\Psi_{\rm initial}$ is

$$\begin{aligned}\langle m\bar{l}|H_I|p\rangle &= \int ds \int d^4x\, \Psi^*_{\rm final}(s,x)\Psi_{\rm initial}(s,x)\\ &\quad\times\langle q\overline{ql}|\psi^4(x)|q^3\rangle_s\\ &\approx\langle q\overline{ql}|\psi^4(x)|q^3\rangle_{s=1,x=0}\mathcal{I},\end{aligned}\tag{1}$$

where ''initial'' means a Skyrmion with topological number one and ''final'' means vacuum with topological number zero. Further,

$$\psi^4=\sum_i\ \bar{\psi}_l\mathcal{O}_{ia}\psi_{qa}\bar{\psi}^c_{qd}\mathcal{O}^i_{db}\psi_{qb}\Gamma^{abd},\tag{2}$$

and

$$\mathcal{I}=\int ds\,\Psi^*_{\rm final}(s)\Psi_{\rm initial}(s)\tag{3}$$

is the inhibition factor due to hadron dynamics that will be calculated in the next section. The integration variable s accounts for the quantum fluctuations (to be defined below in terms of separate scaling variables, $s_{\rm int}$ and $s_{\rm ext}$, for the initial and final state wave functions, respectively). The Ψ's in Eq. (3) do not show an x dependence because that has already been integrated out in the Skyrme model we use, also to be discussed below. However, $\mathcal{I}$ does include a phase factor e^{-iMt}, not shown, because the initial chiral field wave function has the mass of the nucleon, M, while the final (vacuum) wave function has exactly zero energy. This factor assures that the total energy of the final lepton and meson will be the mass of the initial nucleon. The approximate factorization of the amplitude indicated in the last line of Eq. (1) will be justified in Sec. IV.

III. CALCULATION OF INHIBITION FACTOR FROM SKYRMION DYNAMICS

A. Skyrmion profile function

The Skyrme model of the nucleon [5] begins with a Lagrangian

$$\mathcal{L}=\frac{F_\pi^2}{16}\mathrm{Tr}\{\partial_\mu U\partial^\mu U^\dagger\}+\frac{1}{32e^2}\mathrm{Tr}\{[L_\mu,L_\nu]^2\},\tag{4}$$

where $L_\mu=U^\dagger\partial_\mu U$ and the static Skyrmion wave function U is defined as

$$U=e^{i\vec{\tau}\cdot\hat{\mathbf{r}}F(r)}.\tag{5}$$

Here F_π is the pion decay constant, which is fitted at 129 MeV by Adkins, Nappi, and Witten (ANW) [8], smaller than the experimental value of 188 MeV (in the conventions of ANW). The quartic ''Skyrme term'' stabilizes the soliton against collapse; its coefficient has a dimensionless constant e which is fitted at the value 5.45 in ANW.

Extremizing $\mathcal{L}$ to get an ''equation of motion'' for the profile function $F(r)$ yields the nonlinear differential equation

$$\begin{aligned}&\left(\frac{1}{4}r^2+2\sin^2F\right)F''+\frac{1}{2}rF'+\sin 2F\left[(F')^2-\frac{1}{4}\right]\\ &\quad-\frac{\sin^2F}{r^2}\sin 2F=0.\end{aligned}\tag{6}$$

The radial coordinate r here is dimensionless, with the corresponding dimensional coordinate given by $r/(eF_\pi)$.

For a single nucleon (i.e., baryon number $B=1$) Eq. (6) has boundary conditions $F(0)=\pi$ and $F(r)\to a/r^2$ as $r\to\infty$. It turns out that $F'(0)=-1.03812$, falling off linearly from the origin, and the asymptotic constant $a=8.63385$. We shall use variations of $F(r)$ to describe the pion field in the initial state of the decaying nucleon.

Note that if $F(r)$ is a solution of this equation, then so is $\pi-F(r)$. Let R be the point where $F(R)=\pi-F(R)=\pi/2$. [From the solution for $F(r)$, $R=1.76$; for the ANW choice of F_π and e this corresponds to a distance from the origin of 0.49 fm.] Thus we also can create a $B=0$ configuration which solves Eq. (6) by taking the piecewise combination

$$\tilde{F}(r)=\begin{cases}\pi-F(r) & \text{if } r<R,\\ F(r) & \text{otherwise.}\end{cases} \tag{7}$$

This solution is valid except at $r=R$, where the derivative of F is discontinuous. A smoother approximate $B=0$ solution with the constraint $F(R)=\pi/2$ could be obtained easily using Eq. (7) by some rounding in the neighborhood of the cusp at $r=R$. We shall be using $\tilde{F}(r)$ for the contribution to the inhibition factor $\mathcal{I}$ from the $B=0$ final state wave function's chiral field dependence.

The nucleon mass M in the Skyrmion picture [8] is just the value of $\mathcal{L}$ evaluated for the solution $F(r)$:

$$M=M_2+M_4$$

$$M_2=\frac{\pi F_\pi^2}{2}\left(\frac{1}{eF_\pi}\right)\int_0^\infty dr\,[r^2F'^2+2\sin^2F] \tag{8}$$

$$M_4=\frac{2\pi}{e^2}(eF_\pi)\int_0^\infty dr\sin^2F\left[\frac{\sin^2F}{r^2}+2F'^2\right].$$

Because we minimized $\mathcal{L}$ to get F, $M_2=M_4$. Note that both $F(r)$ and $\tilde{F}(r)$ give the same value for M. This means that the $B=0$ state represented by $\tilde{F}$ does not have an energy appropriate to the hadronic part of a final state of, say, a pion and an electron, much less to the energy of the vacuum. This assumes one wishes to describe the final meson as produced from a quark-antiquark pair left by the action of the four-fermion operator on the initial baryon state, rather than by evolution of the classical chiral field represented by $\tilde{F}$.

B. Varying the initial and final state wave functions

The Skyrmion is a classical soliton solution which minimizes the Lagrangian, Eq. (4). We want to allow for quantum fluctuations in the calculation of the ''tunneling'' inhibition factor $\mathcal{I}$, and we do that by making variations of $F(r)$ and $\tilde{F}(r)$. We need to do this differently for the two cases, because of the different boundary conditions to be satisfied, $B=1$ and $B=0$, respectively. We introduce scaling factors $s_{\rm int}$ and $s_{\rm ext}$, respectively, which are allowed to depend on time. The time derivatives of each $s(t)$ in the modified Lagrangian, Eq. (4), then lead to Schrödinger-like equations with potential wells that can be reasonably well approximated by quadratic functions in each s. This then lets us write the initial and final states $\Psi^*_{\rm final}(s_{\rm ext})$ and $\Psi_{\rm initial}(s_{\rm int})$ as harmonic oscillator wave functions. In the end, we can evaluate a simple integral over $s_{\rm ext}$ to get the inhibition factor $\mathcal{I}$.

C. The final state wave function

For purposes of presentation, it is easier to discuss first the scaling of the final state $\tilde{F}$. The $B=0$ boundary condition, that $\tilde{F}$ vanish at both $r=0$ and $r=\infty$, can be simply maintained by letting

$$\tilde{F}(r)\to s_{\rm ext}\tilde{F}(r), \tag{9}$$

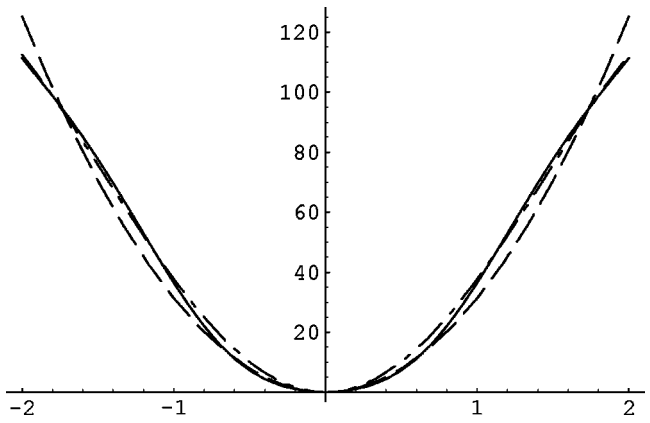

FIG. 1. Plot of $V_{\rm ext}(s_{\rm ext})$ in units of F_π/e (solid curve). The dot-dashed curve is a quartic fit to $V_{\rm ext}(s_{\rm ext})$ and the long-dashed curve is a quadratic fit.

where the subscript ''ext'' refers to scaling external to the functional argument. Substituting this in the Lagrangian of Eq. (4) then gives a ''potential'' $V_{\rm ext}(s_{\rm ext})$ with a minimum at $s_{\rm ext}=0$, as shown in Fig. 1.

The figure shows the calculated $V_{\rm ext}$, which exhibits slight turnovers at $s=\pm1.5$, together with a quartic fit to it (hardly distinguishable) and a quadratic fit (lacking the turnovers). As eventually we shall be interested in values of $s_{\rm ext}$ between 0 and 1, the quadratic fit is adequate for our purposes. The fitted quadratic is

$$V_{\rm ext}(s_{\rm ext})=\frac{1}{2}as_{\rm ext}^2,\quad a=63, \tag{10}$$

with the factor of $\frac{1}{2}$ inserted to mimic the simple harmonic oscillator potential. Here a has units F_π/e.

If we now go on to allow $s_{\rm ext}$ to have a time dependence, the Lagrangian in Eq. (4) leads, in both terms (those quadratic and quartic in derivatives), to a dependence on $\dot{s}_{\rm ext}^2$,

$$\mathcal{L}\to\mathcal{L}(s_{\rm ext})=\frac{1}{2}I_{\rm ext}\dot{s}_{\rm ext}^2+V_{\rm ext}(s_{\rm ext}) \tag{11}$$

$$I_{\rm ext}=\frac{\pi}{e^3F_\pi}\int_0^\infty dr\,r^2\tilde{F}^2(r)\times\left[1+8\frac{\sin^2[s_{\rm ext}\tilde{F}(r)]}{r^2}\right].$$

The $s_{\rm ext}$-dependence of the ''moment of inertia'' $I_{\rm ext}$ is shown in Fig. 2.

The variation of $I_{\rm ext}$ over the range $s_{\rm ext}=0$ to 1 is small, so for simplicity we take it to be a constant, $I_{\rm ext}=135$ in units of $1/e^3F_\pi$.

The ''momentum'' canonical to $s_{\rm ext}$ is $(I_{\rm ext})\dot{s}_{\rm ext}$. Converting $\mathcal{L}$ into a Hamiltonian and replacing the momentum by $-i\partial/\partial s_{\rm ext}$ then gives a Schrödinger-like equation for the final state (vacuum) wave function,

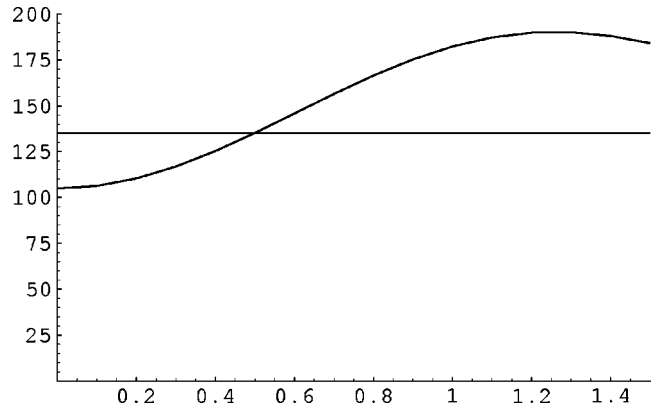

FIG. 2. Plot of $I_{\rm ext}(s_{\rm ext})$ in units of $1/e^3F_\pi$. The horizontal line has a *y*-axis value of 135, which we will take as a constant approximation for $I_{\rm ext}$.

$$\left[-\frac{1}{2I_{\rm ext}}\frac{\partial^2}{\partial s_{\rm ext}^2}+\frac{1}{2}as_{\rm ext}^2\right]\Psi_{\rm ext}(s_{\rm ext})=E\Psi_{\rm ext}(s_{\rm ext}). \quad (12)$$

This equation has the form of the familiar harmonic oscillator problem. We take $\Psi_{\rm final}$ to be the ground state eigenfunction,

$$\Psi_{\rm final}(s_{\rm ext})=N_{\rm ext}\exp(-\alpha_{\rm ext}^2 s_{\rm ext}^2/2), \quad (13)$$

where $\alpha_{\rm ext}^4=$ ''mK'' $=Ia/e^4$. For ANW's $e=5.45$, we get $\alpha_{\rm ext}^2=3.105$ and the normalization constant $N_{\rm ext}^2=\alpha_{\rm ext}/\sqrt{\pi}=0.994$. The ground state eigenvalue is

$$E_0=\frac{1}{2}\sqrt{(a/I)}=0.342 \quad (14)$$

in units of $F_\pi e$, i.e., $\approx$240 MeV, using ANW's fitted values for these coupling constants.

D. The initial state wave function

For the initial state, in making variations of the F we need to maintain the $B=1$ boundary conditions mentioned below Eq. (6). We therefore have chosen simply to introduce another scaling parameter $s_{\rm int}$ so that

$$F(r)\to F(s_{\rm int}r), \quad (15)$$

where the subscript ''int'' refers to scaling internal to the function $F(r)$. It will turn out that the scaling variable here, $s_{\rm int}$, is not quite what is needed for the integration over s in Eq. (1), which we choose in Eq. (3) to be the $s_{\rm ext}$ defined in the last sub-section. The relation between the two scaling variables will be dealt with below.

Using $F(s_{\rm int}r)$ we can define a ''potential'' for the initial state wave function from the expression for the nucleon mass, Eq. (8):

$$V_{\rm int}(s_{\rm int})=M[F(s_{\rm int}r)]=M_2/s_{\rm int}+M_4 s_{\rm int}. \quad (16)$$

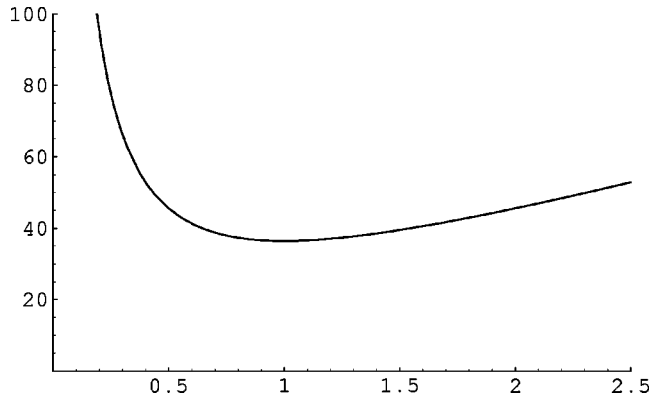

FIG. 3. Plot of $V_{\rm int}(s_{\rm int})$ around $s_{\rm int}=1$ in units of F_π/e.

This simple $s_{\rm int}$-dependence can be understood by replacing r, the variable of integration in Eq. (8), by $r'=s_{\rm int}r$. Figure 3 shows that $V(s_{\rm int})$ has a shallow minimum at $s_{\rm int}=1$, as it should.

Again, we let $s_{\rm int}$ have a time dependence and find the modified Lagrangian to be

$$\mathcal{L}\to\mathcal{L}(s_{\rm int})=\frac{1}{2}I_{\rm int}(s_{\rm int})\dot{s}_{\rm int}^2+V_{\rm int}(s_{\rm int}), \quad (17)$$

$$I_{\rm int}(s_{\rm int})=I_{{\rm int},2}(s_{\rm int})+I_{{\rm int},4}(s_{\rm int}), \quad (18)$$

$$I_{{\rm int},2}(s_{\rm int})=\frac{\pi}{e^3F_\pi}\int_0^\infty dr\, r^4\tilde{F}'^2(s_{\rm int}r), \quad (19)$$

$$I_{{\rm int},4}(s_{\rm int})=\frac{4\pi}{e^3F_\pi}\int_0^\infty dr\, r^2\tilde{F}'^2(s_{\rm int}r)\times\sin^2[\tilde{F}(s_{\rm int}r)]\times\{1+2\sin^2[\tilde{F}(s_{\rm int}r)]\}. \quad (20)$$

Note that $I_{{\rm int},2}$'s integrand has a slow fall-off in r, which necessitates some care in calculating the contribution of the asymptotic tail. By the same change of integration variable as for $V_{\rm int}$ we see that

$$I_{\rm int}(s_{\rm int})=I_{{\rm int},2}(1)/s_{\rm int}^5+I_{{\rm int},4}(1)/s_{\rm int}^3. \quad (21)$$

Evaluating the integrals in Eq. (18), we find $I_{{\rm int},2}(1)=110.46$ and $I_{{\rm int},4}(1)=46.86$.

One might worry that $I_{\rm int}$ is a steeply falling function of $s_{\rm int}$. However, as already mentioned, we shall be doing the final integration in Eq. (3) over $s_{\rm ext}$. Thus we need the relation between the two scaling variables, which is

$$s_{\rm ext}=\frac{2}{\pi}F(s_{\rm int}R). \quad (22)$$

This relation also defines, implicitly, $s_{\rm int}$ as a function of $s_{\rm ext}$. Note that as $s_{\rm int}$ runs from 0 to 1 to ∞, $s_{\rm ext}$ falls from 2 to 1 to 0. From Eq. (22) we also have

$$\frac{ds_{\rm ext}}{dt}=\frac{2R}{\pi}\left[\frac{dF(r)}{dr}\right]_{r=s_{\rm int}R}\frac{ds_{\rm int}}{dt}. \quad (23)$$

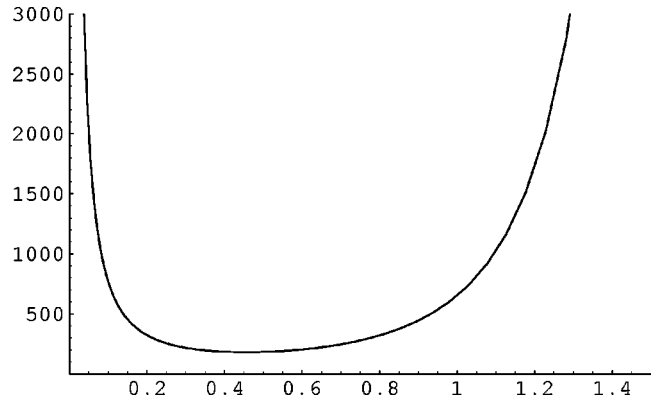

FIG. 4. Plot of X as a function of $s_{\rm ext}$ in units of $1/e^3F_\pi$.

We need this last relation, Eq. (23), for converting the ''kinetic energy'' term in Eq. (17). With it, the moment of inertia term as a function of $s_{\rm ext}$ becomes

$$\frac{1}{2}I_{\rm int}(s_{\rm int})\dot{s}_{\rm int}^2=\frac{1}{2}X(s_{\rm int})\left(\frac{ds_{\rm ext}}{dt}\right)^2, \tag{24}$$

$$X(s_{\rm ext})=\left(\frac{\pi}{2R}\right)^2\left[\frac{1}{dF(s_{\rm int}R)/dr}\right]^2 I_{\rm int}(s_{\rm int}), \tag{25}$$

where Eq. (22) is used to convert the variable $s_{\rm int}$ to $s_{\rm ext}$. Since $F'(s_{\rm int}R)$ falls off like $1/s_{\rm int}^3$ at large $s_{\rm int}$, the $1/F'^2$ factor more than compensates the $1/s_{\rm int}^3$ falloff of $I_{\rm int}(s_{\rm int})$ seen in Eq. (21). Thus $X(s_{\rm ext})$ is a steep-sided, somewhat flat-bottomed well (shown in Fig. 4) instead of a steeply falling function.

Below we shall replace $X(s_{\rm ext})$ by a constant, X_0, which we take as its value over the flat bottom. $X_0\approx 300$ in units of $1/e^3F_\pi$. This is a reasonable approximation in that the wave function we are trying to find, $\Psi_{\rm initial}$, will be exponentially small in the regions where $X(s_{\rm ext})$ is large.

In addition to the kinetic energy term, we also need to convert the potential term into a function of $s_{\rm ext}$. This also undergoes a dramatic change of form from that in Fig. 3, as shown in Fig. 5.

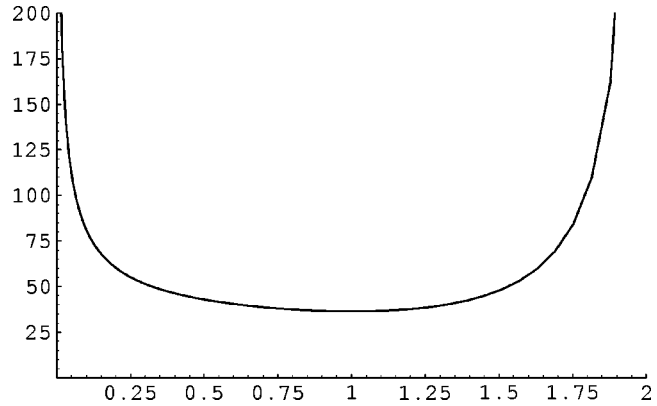

FIG. 5. Plot of $V_{\rm int}(s_{\rm int})$ as a function of $s_{\rm ext}$ in units of F_π/e.

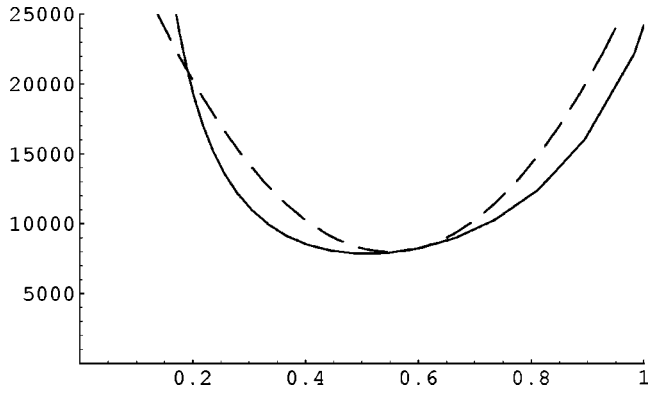

FIG. 6. Plot of XV as a function of $s_{\rm ext}$ (solid curve), compared with the quadratic fit (dashed curve) described in the text.

$V_{\rm int}(s_{\rm int})$ still has its minimum at $s_{\rm ext}=s_{\rm int}=1$, as it must. The steep rise near $s_{\rm ext}=2$ reflects the $1/s_{\rm int}$ falloff near $s_{\rm int}=0$. The rise near $s_{\rm ext}=0$ results from $s_{\rm ext}\sim s_{\rm int}^{-2}$ as $s_{\rm int}$ gets large. That is, for small $s_{\rm ext}$, the linear growth of $V_{\rm int}$ in $s_{\rm int}$ for large $s_{\rm int}$ turns into $s_{\rm ext}^{-1/2}$ behavior near $s_{\rm ext}=0$.

As in the last section, we can now convert the modified Lagrangian in Eq. (17) into a Hamiltonian and thence into a Schrödinger-like equation for the initial-state wave function $\Psi_{\rm initial}$,

$$\left[-\frac{1}{2X(s_{\rm ext})}\frac{\partial^2}{\partial s_{\rm ext}^2}+V_{\rm int}(s_{\rm ext})\right]\Psi_{\rm int}(s_{\rm ext}) =E\Psi_{\rm int}(s_{\rm ext}). \tag{26}$$

We can recast Eq. (26) into an (approximate) harmonic oscillator equation on multiplying up the $X(s_{\rm ext})$ and approximating $X(s_{\rm ext})E\Psi_{\rm int}(s_{\rm ext})$ by $X_0E\Psi_{\rm int}(s_{\rm ext})$. The product of $X(s_{\rm ext})V_{\rm int}(s_{\rm ext})$ is shown as the solid curve in Fig. 6. It looks a little lopsided, but we can find an approximate quadratic fit to XV as

$$X(s_{\rm ext})V_{\rm int}(s_{\rm ext})\approx\left[b+\frac{1}{2}c(s_{\rm ext}-\bar{s})^2\right] \tag{27}$$

with $b=8000$, $c=200\,000$ in units of $1/e^4$ and $\bar{s}=0.55$. The quality of this fit is shown in Fig. 6.

The constant term b just represents a shift in energy, so we want the solution to

$$\left[-\frac{1}{2}\frac{\partial^2}{\partial s_{\rm ext}^2}+\frac{1}{2}c(s_{\rm ext}-\bar{s})^2\right]\Psi_{\rm int}(s_{\rm ext}) =X_0E\Psi_{\rm int}(s_{\rm ext}). \tag{28}$$

As before, we take $\Psi_{\rm initial}$ to be the ground state eigenfunction,

$$\Psi_{\rm initial}(s_{\rm ext})=N_{\rm int}\exp(-\alpha_{\rm int}^2(s_{\rm ext}-\bar{s})^2/2), \tag{29}$$

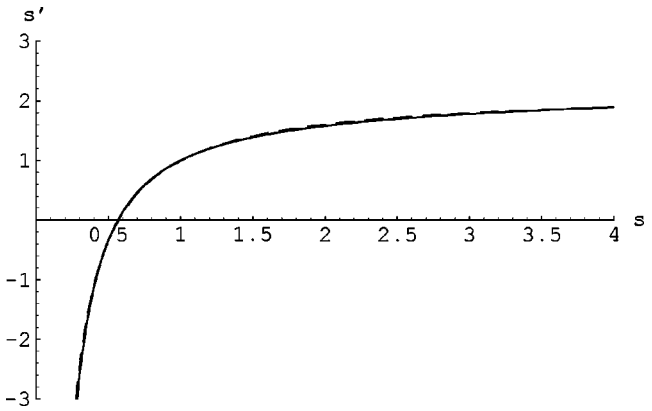

FIG. 7. Plot of s' as a function of $s=s_{\rm int}$, compared with its hyperbolic fit (dashed curve).

where $\alpha_{\rm int}^4=$"mK" $=c/e^4$. For ANW's $e=5.45$, we get $\alpha_{\rm int}^2=15.06$ and the normalization constant $N_{\rm int}^2=\alpha_{\rm int}/\sqrt{\pi}=2.189$.

E. Calculating the overlap integral

With the wave functions given in Eqs. (13) and (29), the integral over $s=s_{\rm ext}$ in the definition of the inhibition factor $\mathcal{I}$, Eq. (3), can be readily evaluated to give

$$\mathcal{I}=\sqrt{\frac{2\alpha_{\rm ext}\alpha_{\rm int}}{\alpha_{\rm ext}^2+\alpha_{\rm int}^2}}\exp\left[-\frac{\alpha_{\rm ext}^2\alpha_{\rm int}^2}{2(\alpha_{\rm ext}^2+\alpha_{\rm int}^2)}\bar{s}^2\right]. \tag{30}$$

With the values of $\alpha_{\rm ext}$, $\alpha_{\rm int}$, and $\bar{s}$ obtained above for the ANW choices of F_π and e, this evaluates to

$$\mathcal{I}=0.588. \tag{31}$$

F. The initial state wave function, reconsidered

When we first saw the result for $\mathcal{I}$ given in the last section, it was a major surprise. We had expected the value to be quite a bit smaller, even if not so small as indicated in Ref. [3]. Thus, we felt compelled to calculate the initial state wave function $\Psi_{\rm initial}$ in a second, more systematic way.

Let us convert the first term of Eq. (17) to something more tractable by defining a new variable s' so that

$$I_2\left(\frac{ds'}{dt}\right)^2=I_{\rm int}\left(\frac{ds_{\rm int}}{dt}\right)^2\equiv I_2\ g(s_{\rm int})\left(\frac{ds_{\rm int}}{dt}\right)^2, \tag{32}$$

where

$$g(s)=[1+\lambda s^2]/s^5,\quad \lambda=I_{{\rm int},4}/I_{{\rm int},2}=0.4242. \tag{33}$$

As a function of $s_{\rm int}$, s' is then given by

$$s'(s_{\rm int})=\int_1^{s_{\rm int}}\sqrt{g(s)}\ ds, \tag{34}$$

with $s'=1$ when $s_{\rm int}=1$. A plot of $s'(s_{\rm int})$ is shown in Fig. 7.

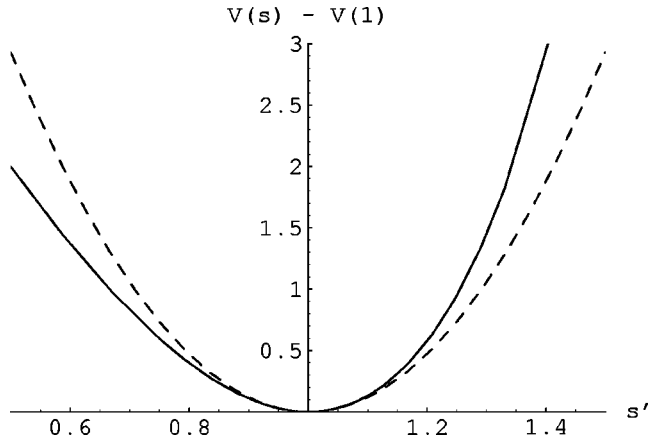

FIG. 8. Plot of $V[s_{\rm int}(s')]-V[s'=1]$ around $s'=1$. Units are in F_π/e. The dashed curve is a quadratic fit.

Note that s' asymptotes to 2.55. It can be fit well with a hyperbola,

$$s'(s_{\rm int})=a+b/(s_{\rm int}-c), \tag{35}$$

where $a=2.167$, $b=-1.093$, and $c=0.06351$. This fit is easily inverted to find $s_{\rm int}$ as a function of s',

$$s_{\rm int}(s')=c+b/(s'-a). \tag{36}$$

The fits in Eqs. (35) and (36) are, because of the singularities at $s'=a$ and $s_{\rm int}=c$, only valid over a limited range between the singularities. This is not a serious problem as we are only interested in variations of $F(r)$ around $s'=s_{\rm int}=1$. As s' runs, say, from 0 to 2, $s_{\rm int}$ varies from 0.5678 to 6.612, steeply rising near $s'=2$.

We are now in a position to write a Schrödinger-like equation for $\Psi_{\rm int}$ in terms of the s' variable,

$$\left\{-\frac{1}{2I_2}\frac{d^2}{ds'^2}+V_{\rm int}[s_{\rm int}(s')]\right\}\Psi_{\rm int}(s')=E\Psi_{\rm int}(s'). \tag{37}$$

The function $V_{\rm int}[s_{\rm int}(s')]$ has a shallow nonsymmetrical minimum at $s'=1$, as shown in Fig. 8.

Let us once again fit $V(s')$ to a quadratic [by evaluating the second derivative of $1/s_{\rm int}(s')+s_{\rm int}(s')$ with respect to s'], finding

$$V_{\rm int}[s_{\rm int}(s')]=V(1)+\frac{1}{2}K_{\rm int}(s'-1)^2, \tag{38}$$

where $K_{\rm int}=2\times 0.644M_2=23.44$, in units of F_π/e, about a third of the "spring constant" for the final state. This fit is shown as the dashed curve in Fig. 8. We then approximate the ground state solution to Eq. (37) as

$$\Psi_{\rm int}(s')=N_{\rm int}e^{-\alpha'^2(s'-1)^2/2}\ \text{for}\ 0\leqslant s'\leqslant 2, \tag{39}$$

and we take $\Psi_{\rm int}(s')$ equal to 0 outside that range. Here $\alpha'^4=I_2K_{\rm int}/e^4$ so $\alpha'^2=1.721$ for ANW's value of e. This value is about half that for $\alpha_{\rm ext}$ found in Sec. III C, meaning

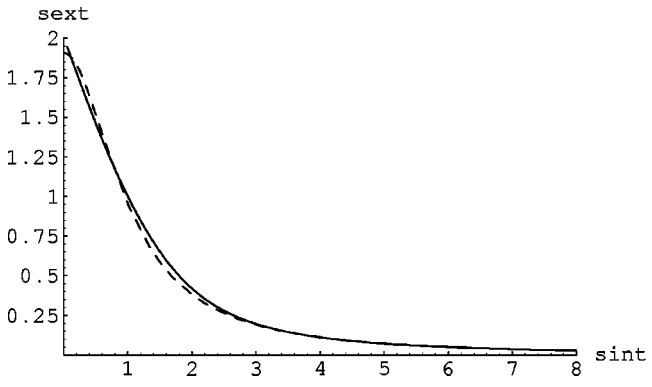

FIG. 9. Plot of $s_{\rm ext}$ as a function of $s_{\rm int}$, compared with the fit described in the text (dashed curve).

that the initial state is ''softer'' than the final state. The Gaussian in Eq. (39) has fallen to 42% of its peak value at the ''end points'' $s'=0$ and 2. The normalization constant $N_{\rm int}$ is determined by integrating the square of $\Psi_{\rm int}(s')$ over the range where it is nonzero, and it turns out to be 0.889. The ground state eigenvalue for this initial state wave function is

$$E_0=\frac{1}{2}\sqrt{K_{\rm int}/I_2}=0.230, \tag{40}$$

again in units of $F_\pi e$. Thus, $E_0\approx 160$ MeV, using ANW's fitted values for these coupling constants.

G. Calculating the overlap integral, part II

With the wave functions given in Eqs. (13) and (39), the integral over $s_{\rm ext}$ in the definition of the inhibition factor $\mathcal{I}$ is a bit trickier to evaluate. We shall do the integration this time using the s' variable, which requires knowing how $s_{\rm ext}$ varies as a function of s'.

From Eq. (22) we show in Fig. 9 how $s_{\rm ext}$ varies as a function of $s_{\rm int}$.

One sees that $s_{\rm ext}$ falls from 2 at $s_{\rm int}=0$ to 0 (as $s_{\rm int}^{-2}$) when $s_{\rm int}$ gets large. Thus a reasonable fit (the dashed curve in Fig. 9) is given by

$$s_{\rm ext}=1.9065/(1+s_{\rm int}^2). \tag{41}$$

Using the fits in Eqs. (35) and (41), we can now evaluate the overlap integral numerically over the range where $\Psi_{\rm initial}$ is defined,

$$\mathcal{I}=\int_0^2 \Psi^*_{\rm final}\{s_{\rm ext}[s_{\rm int}(s')]\}\Psi_{\rm initial}(s')\,ds'=0.4975. \tag{42}$$

We consider this result to be in substantial agreement with (and corroborating) the value for $\mathcal{I}$ found in Sec. III E.

IV. THE HYPOWEAK MATRIX ELEMENT

The hypoweak interaction matrix element is the first factor in the second line of Eq. (1), the matrix element of the operator in Eq. (2). This has been evaluated for chiral vector-axial combinations in terms of the wave function at the origin, providing a flux factor for the two quark to lepton plus antiquark scattering amplitude. As such, the only change needed from previous work [9] is the change in value due to the change in the standing wave for the quark interior between the MIT bag models used earlier (with zero chiral angle) and the constant wave functions appropriate to our new chiral boundary condition. The wave-function factor becomes

$$\frac{j_0^2(0)+j_1^2(0)}{N^2}=\frac{3}{4\pi R^3} \tag{43}$$

where N is the normalization and the spherical Bessel functions of the MIT bag are replaced by a constant from the fermion upper wave-function component and zero from the lower.

Scaling from the result in Ref. [9], where $|\psi(0)|^2=1.1\times 10^{-3}$ GeV^2 was used, to the value here with $R=0.6$ fm, we find an enhancement factor of 7.7, which more than compensates for the overlap suppression from $\mathcal{I}$.

For the intermediate case of a boundary condition chiral angle of $\pi/4$, we need the appropriate frequency for the quark wave-function solution. We need to solve

$$2j_0(\omega R)j_1(\omega R)\tan(\theta_c)=[j_0(\omega R)]^2-[j_1(\omega R)]^2, \tag{44}$$

which gives the value $\omega R=1.7446$ for

$$\theta_c=\pi-\theta(R)+\frac{\sin[2\,\theta(R)]}{2}. \tag{45}$$

Evaluating the usual normalization integral, we find

$$\omega^3 N(\omega)^2=4\pi\int_0^{\omega R} dx\,x^2\{[j_0(x)]^2+[j_1(x)]^2\}$$
$$=14.935. \tag{46}$$

Equation (43) then becomes

$$\frac{j_0^2(0)+j_1^2(0)}{N^2(\omega)}=\frac{5.3096}{14.935R^3}. \tag{47}$$

This produces an enhancement factor almost three times smaller than above, but still implies that for the net matrix element including the tunneling overlap factor $\mathcal{I}$ there is no major change from the original MIT bag calculation.

V. CONCLUSIONS

The fact that hadronic suppression of baryon decay *could* be much less significant than suggested in Ref. [3] had become clear to us some time ago, but we still were surprised to find virtually no suppression. It should be emphasized that Ref. [3] did not assert that the suppression would be large, only noting that an exponential amplitude suppression factor exhibiting a negative exponent with order of magnitude unity could easily account for two orders of magnitude reduction

in the decay rate. What has developed in our much more detailed calculation above is that several effects serve to weaken this potential suppression. First, the size of the vacuum fluctuations, when examined more carefully, turns out to be larger than simple dimensional counting suggested. Secondly, the initial nucleon wave function as well as the final vacuum wave function allow substantial local fluctuations in baryon density, so that the overlap between the former (once acted on by the four-fermion operator) and the latter can be rather large. Thirdly, the four-fermion matrix element becomes larger when one considers the initial quarks as confined in a smaller bag than the MIT bag.

The net effect, within the remaining uncertainties in the calculations, is that the present more elaborate analysis used here produces virtually the same prediction as that in the MIT bag model. This might be one more example of the ''Cheshire-cat'' phenomenon [10,6], that many properties of the nucleon are quite insensitive to the choice of demarcation radius between a chiral field description (used outside that radius) and a description in terms of quarks (inside), subject to an appropriate chiral boundary condition. If so, then even the decay of the proton may not reveal what lies inside it, instead quite directly measuring the microscopic operator behind the decay.

In this work we have not focused on the matrix element for production of the final meson from the remaining quark and the produced antiquark. Independently of the hybrid bag picture, this might be a worthwhile subject for additional study, and probably is the largest source of remaining uncertainty in the lifetime calculation. Assuming this also does not produce a large effect, then the latest quoted limits on both the old $e^+\pi^0$ and new $\bar{\nu}K^+$ favored channels for proton decay already provide ominous constraints on grand unified models [11].

Note added in proof. It is worth recalling that a very different approach from that in this paper, namely, lattice QCD with fermions treated in quenched approximation as studied by the JLQCD Collaboration [12], also gives large decay rates—further supporting extension of the ''Cheshire-cat'' concept to baryon decay.

ACKNOWLEDGMENTS

Shmuel Nussinov was an active partner in the early stages of this work, and he was the first to suggest that a more careful look might reveal much less substantial hadronic suppression of baryon decay than the old, but crude, arguments had indicated. Our further efforts have more than vindicated that view. This research is supported in part by the Department of Energy under contract W-7405-ENG-36 (T.G. and R.R.S.) and the National Science Foundation under grant PHY00-71018 (A.S.G.).

[1] Super-Kamiokande Collaboration, S. Fukuda *et al.*, Phys. Rev. Lett. **86**, 5656 (2001).
[2] SNO Collaboration, Q.R. Ahmad *et al.*, Phys. Rev. Lett. **87**, 071301 (2001).
[3] A.S. Goldhaber, T. Goldman, and S. Nussinov, Phys. Lett. **142B**, 47 (1984).
[4] A recent example is K.S. Babu, J.C. Pati, and F. Wilczek, Nucl. Phys. **B566**, 33 (2000).
[5] T.H.R. Skyrme, Proc. R. Soc. London **A260**, 127 (1961).
[6] G.E. Brown and M. Rho, Phys. Lett. **82B**, 177 (1979); M. Rho, A.S. Goldhaber, and G.E. Brown, Phys. Rev. Lett. **51**, 747 (1983); J. Goldstone and R.L. Jaffe, *ibid.* **51**, 1518 (1983).
[7] A. Chodos, R.L. Jaffe, K. Johnson, C.B. Thorn, and V.F. Weisskopf, Phys. Rev. D **9**, 3471 (1974).
[8] G.S. Adkins, C. Nappi, and E. Witten, Nucl. Phys. **B228**, 552 (1983). We will refer to this reference as ANW.
[9] T.J. Goldman and D.A. Ross, Nucl. Phys. **B171**, 273 (1980).
[10] S. Nadkarni and H.B. Nielsen, Nucl. Phys. **B263**, 1 (1986).
[11] Uno Project white paper: http://ale.physics.sunysb.edu/nngroup/uno/
[12] JLQCD Collaboration, S. Aoki *et al.*, Phys. Rev. D **62**, 014506 (2000).